Discrimination between Enantiomers of Structurally Related Molecules: Separation of Benzodiazepines by Molecularly Imprinted Polymers

Bradley R. Hart, Daniel J. Rush, and Kenneth J. Shea*

Contribution from the Department of Chemistry, University of California, Irvine, California 92697-2025

Received July 26, 1999

Abstract: Molecular imprinting has been used to create synthetic receptor sites for a series of chiral benzodiazepines. A detailed HPLC analysis of binding properties using molecularly imprinted polymers (MIPs) as the stationary phase showed that binding, as measured by chromatographic retention, shows significant dependence on the chiral match or mismatch. In addition, the shape and spatial orientation of functionality of the imprinted binding site is also critical for recognition. Imprinted polymers, therefore, are not only able to discriminate between enantiomers of the imprinted molecule, they also demonstrate an ability to discriminate between a wide range of enantiomers of structurally related molecules that have not been imprinted. The ability of MIPs to discriminate between enantiomers of molecules in favor of the imprinted absolute configuration, even as the structural homology between the enantiomers and the original template decreases, indicates that the synthetic benzodiazepine receptors may serve as crude mimics of the natural receptor.

The separation of enantiomers by molecularly imprinted polymers (MIPs) has proven to be one of the more challenging and exciting applications of this growing technology.[1] Additionally, the use of MIPs for drug assays[2,3] and as sensors[3,4] is an area of considerable research effort. We report the use of molecular imprinting to create materials capable of shape selective chiral recognition of benzodiazepine derivatives. Of special significance is that, while these materials are able to discriminate between enantiomers of the imprinted molecule, they also demonstrate the ability to discriminate between a wide range of enantiomers of structurally related molecules that have not been imprinted. The ability to resolve enantiomers of a family of molecules in favor of the imprinted absolute configuration follows trends that can be understood in terms of rational concepts that control recognition in molecular imprinting.[5] This insight along with complimentarity of functionality can lead to the creation of "designer" recognition sites that may ultimately have the capability to sort molecules on the basis of their physiological activity.[2,3]

Benzodiazepines are a class of compounds that modify affective responses to sensory perceptions. Their action results from modulating the GABA system in the brain via specific benzodiazepine receptors that form an integral part of the $GABA_A$ receptor−chloride channel complex. The exact structure of native $GABA_A$ receptor subtypes remains unknown, and there has been no assignment of receptor subtypes to particular behaviors or pathologies.[6] Due to this lack of information about the receptors involved in benzodiazepine action, we set out preparing synthetic receptors for this class of molecule. To this end we have synthesized a series of imprinted polymers using a family of structurally related chiral benzodiazepines as templates. These materials were then examined to determine their ability to resolve enantiomers of benzodiazepines with varying structures.

Scheme 1

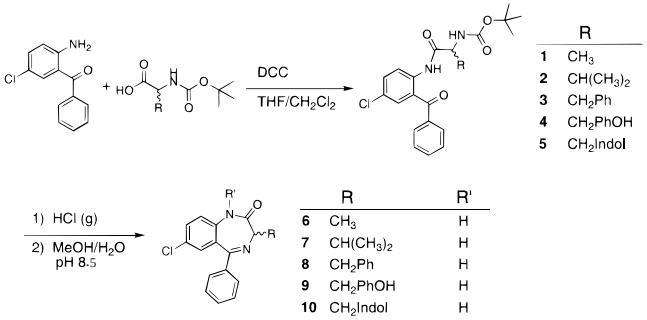

	R
1	CH_3
2	$CH(CH_3)_2$
3	CH_2Ph
4	CH_2PhOH
5	CH_2Indol

	R	R'
6	CH_3	H
7	$CH(CH_3)_2$	H
8	CH_2Ph	H
9	CH_2PhOH	H
10	CH_2Indol	H

Enantiomerically pure benzodiazepines **6**−**10** were synthesized from L- and D-alanine, valine, phenylalanine, tyrosine, and tryptophan by the procedure outlined in Scheme 1.[7]

(1) (a) Sellergren, B.; Shea, K. J. *J. Chromatogr. A* **1993,** *635,* 31−49. (b) Mosbach, K. *Trends Biol. Sci.* **1994,** *19,* 9−14. (c) Kempe, M. *Anal. Chem.* **1996,** *68,* 1948−1953. (d) Ramstrom, O.; Ansell, R. *Chirality* **1998,** *10,* 195−209. (e) Remcho, V. T.; Tan, Z. J. *Anal. Chem.* **1945**, *17,* 248A-255A. (f) *Molecular and Ionic Recognition with Imprinted Polymers;* Bartsch, A., Maeda, M., Eds.; ACS Symp. Ser. 703; American Chemical Society: Washington, DC, 1998.

(2) (a) Vlatakis, G.; Andersson, L. I.; Muller, R.; Mosbach, K. *Nature* **1993**, *361,* 645−647. (b) Ramstrom, O.; Ye, L.; Krook, M.; Mosbach, K. *Anal. Commun.* **1998**, *35,* 9−11. (c) Karlsson, P. K. O.; Lutz, E. S. M.; Andersson, L. I *Trends Anal. Chem.* **1999**, *18,* 146−154.

(3) Haupt, K.; Mosbach, K. *Trends Biol. Sci.* **1998**, *16,* 468−475.

(4) (a) Kriz, D.; Ramstrom, O.; Mosbach, K. *Anal. Chem.* **1997**, *69,* A345−A349. (b) Arnold, B. R.; Euler, A. C.; Jenkins, A. L.; Uy, O. M.; Murray, G. M. *Johns Hopkins APL Tech. Digest* **1999**, *20,* 190−197. (c) Yano, K.; Karube, I. *Trends Anal. Chem.* **1999**, *18,* 199−204.

(5) (a) Spivak, D.; Gilmore, M. A.; Shea, K. J. *J. Am. Chem. Soc.* **1997**, *119,* 4388−4393. (b) Sellergren, B. *Trends Anal. Chem.* **1999**, *3,* 164−174.

(6) (a) Hobbs, W.; Rall, T.; Verdoorn, T. In *Goodman & Gillman's The Pharmaceutical Basis of Therapeutics*, 9th ed.; Hardman, J., Limbird, L., Eds.; McGraw-Hill: New York, 1996, Chapter 17. (b) Braestrub, C.; Nielsen, M.; Honore, T.; Jensen, L. H.; Petersen, E. N. *Neuropharmacology* **1983**, *22,* 1451−1457. (c) Takeuchi, T.; Tanaka, S.; Rechnitz, G. A. *Anal. Biochem.* **1992**, *203,* 158−162.

(7) Sunjie, v.; Kajfez, F.; Stromar, I.; Blazevic, N.; Kolbah, D. *J. Hetercycl. Chem.* **1973**, *10,* 591.

10.1021/ja9926313 CCC: $19.00
Published on Web 12/31/1999

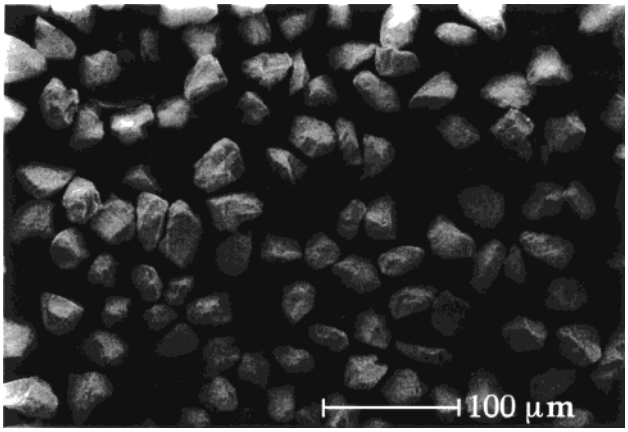

Figure 1. SEM image of 25−38 μm MIP particles. Surface area and pore analysis indicate that these materials have an average surface area of 256 m^2/g, and an average pore diameter of 94 Å.

Table 1. Benzodiazepine α Values for Retention on MIP Stationary Phases[a,b]

	benzodiazepine derivative injected				
MIP template	4-hydroxy-benzyl (**9**)	benzyl (**8**)	indolyl (**10**)	isopropyl (**7**)	methyl (**6**)
a. ***S*-9** 4-hydroxybenzyl	3.8	2.5	1.3	1.6	1.4
b. ***S*-8** benzyl	2.3	3.0	1.7	1.6	1.7
c. ***S*-10** indolyl	1.5	1.8	2.3	1.3	1.4
d. ***S*-7** isopropyl	1.2	1.3	1.3	2.2	1.6
e. ***S*-6** methyl[c]	1.0	1.1	1.1	1.1	1.3

[a] Photochemically initiated polymer with acetonitrile used as the porogen. [b] HPLC performed using acetonitrile as eluent. [c] A MIP prepared using the opposite enantiomer, ***R*-6**, showed selectivity in favor of the (R) enantiomers which was slightly higher than the data shown.

Individual benzodiazepine derivatives ***S*-6** through ***S*-10** were subsequently used to imprint ethylene glycol dimethacrylate (EGDMA) polymers using methacrylic acid (MAA) as the functional monomer. Solutions of template (1%), MAA (11%), EGDMA (87%), and AIBN (1%) in acetonitrile were polymerized photochemically by UV irradiation for 12 h while immersed in a circulating bath at 0 ± 2 °C. The resulting polymers were crushed, extracted with methanol, ground, and sieved to a 25−38 μm particle size (Figure 1). These particles were slurry packed in 10 cm × 0.46 cm i.d. stainless steel chromatography columns for evaluation by HPLC.[5]

Solutions of enantiomerically pure benzodiazepine derivatives were injected onto HPLC columns containing MIP stationary phases imprinted with the *S*-enantiomer of a benzodiazepine derivative. Corrected retention volumes (capacity factors, k')[8] were calculated against a void volume marker (acetone) and the ratios of the k' values for each enantiomeric pair ($\alpha = k'_S/k'_R$) are summarized in Table 1. The α values across each row show the ability of a specific MIP to resolve a series of benzodiazepine enantiomers. The α values in each column indicate how a particular benzodiazepine is resolved on the series of MIPs.

Looking across the rows in Table 1, one observes that each *S*-MIP is most selective for the *S*-enantiomer over the *R* regardless of the imprint molecule ($\alpha > 1$). Additionally, the *highest* α value in each row corresponds to that of the *imprinted* benzodiazepine (bold entries). We would anticipate this result in that an imprinted void within the MIP should selectively bind molecules that have the best size, shape, and functional group complementarity. In the absence of competing effects, a molecule that has a superior "fit" at the site should be retained longer by the MIP stationary phase. For enantiomers, this diastereomeric cavity/molecule interaction is the only discriminating factor. The ability of benzodiazepine MIPs to produce high α values for a family of molecules in favor of the absolute configuration of the template is an important result of this study. In addition, the recognition sites created by imprinting reflect not only the chirality of the microenvironment, but also the shape and functional group complimentarity of the sites (Figure 2).

It was found that as structural similarity between the imprint molecule and the analyte molecule diminishes, both retention and selectivity decrease. In our study, this was explored by modifying the side chains at the asymmetric center and observing the resulting changes in the α values.

More specifically, the MIP made from the ***S*-6** benzodiazepine (methyl derivative) showed low α values for all nonmethyl derivatives (row e). If one focuses on the steric environment at the chiral center, the methyl group of ***S*-6** will create an imprinted "void" in the polymer cavity that should be too small to accommodate any of the other side chains studied. We see this expressed as moderate selectivity for enantiomers of template **6** and negligible selectivity for the other benzodiazepine derivatives.

This situation is not likely true for binding sites created by benzodiazepines containing larger R groups at the asymmetric center. The ***S*-9** benzodiazepine (4-hydroxy benzyl derivative) MIP is illustrative in this case because the imprinted cavity should be large enough to accommodate most of the other side chains. Discrimination between enantiomers of benzodiazepine **9** is high, $\alpha = 3.8$ (row a). Making a relatively small perturbation to the analyte by removing the aromatic hydroxyl group results in a *lower*, but still significant, separation factor of $\alpha = 2.5$. The α values continue to erode for the remaining derivatives in reasonable order of how well each of the *S*-enantiomers should be accommodated at the binding site based on the relative van der Waals volume of the side chains.[9]

This analysis can also be used to explain the other trends in Table 1. The ***S*-7** MIP might be expected to have a slightly larger binding site based on the van der Waals volume of the side chains than the ***S*-6** MIP and, therefore, it can accommodate ***S*-7** and ***S*-6**, but not the larger residues (row d). In the ***S*-10** benzodiazepine (indolyl derivative) imprinted polymers, the erosion of α presumably stems from a non-optimal fit and noncomplementarity of the slightly smaller aromatic residues (row c). The lower α for analytes **6** and **7** stems perhaps from these residues having too much freedom at the ***S*-10** imprinted binding site to produce the best chiral discrimination. This MIP presents a case where the large binding site is shaped uniquely enough that none of the other residues exhibit high selectivity in binding, but because the smaller side chains can be accommodated, some chiral preference is observed, unlike with the ***S*-6** MIP. Similarly, the ***S*-8** benzodiazepine (benzyl derivative) MIP creates a cavity that roughly accommodates ***S*-9**, but does not discriminate well among the other derivatives. The side chain of ***S*-10** is too big to be accommodated in the recognition site, while the smaller sizes of the ***S*-6** and ***S*-7** side chains result in lowered α values (row b).

We can understand the retention and selectivity data as the result of both specific and nonspecific interactions of analyte

(8) The capacity factor (k') is defined as $k' = [(V(t) - V(0))/V(0)]$, where $V(t)$ is the retention volume and $V(0)$ is the dead volume or the retention volume of a nonbinding substrate. The 95% confidence limits were calculated for all capacity factors and separation factors. For the capacity factors, all confidence limits were equal to or less than ±0.06. For separation factors, all confidence limits were equal to or less than ±0.1.

(9) Creighton, T. E. *Proteins Structures and Molecular Properties*, 2nd ed.; W. H. Freeman & Co.: New York, 1993; Chapter 1.

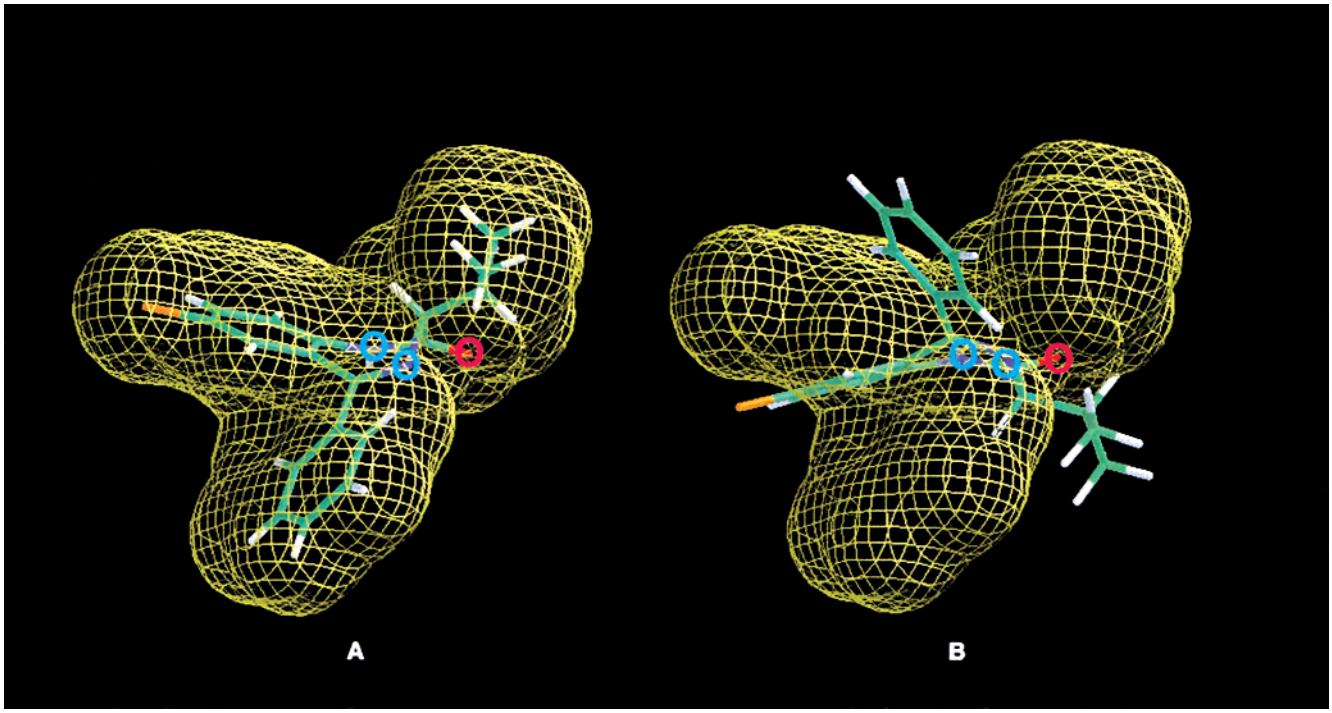

Figure 2. (A) Receptor site simulated by the density surface of an X-ray crystal structure of *S*-(**7**). (B) An attempted "fit" of *R*-(**7**) in the simulated receptor site. The orientation of *R*-(**7**) was chosen so as to maintain the position of the carbonyl oxygen (red circle) and the amide NH and imine nitrogen (blue circles) in both enantiomers.

Table 2. Benzodiazepine Capacity Factors for Retention on MIP Stationary Phases[a,b]

	benzodiazepine derivative injected									
	4-hydroxybenzyl (**9**)		benzyl (**8**)		indolyl (**10**)		isopropyl (**7**)		methyl (**6**)	
MIP template	k'_R	k'_S	k'_R	k'_S	k'_R	k'_S	k'_R	k'_S	k'_R	k'_S
a. ***S*-9** 4-hydroxybenzyl	0.33	1.25	0.27	0.68	0.48	0.62	0.27	0.43	0.38	0.53
b. ***S*-8** benzyl	0.44	0.99	0.38	1.15	0.47	0.82	0.32	0.52	0.44	0.75
c. ***S*-10** indolyl	0.51	0.79	0.43	0.76	0.57	1.31	0.42	0.54	0.52	0.70
d. ***S*-7** isopropyl	0.23	0.26	0.22	0.29	0.27	0.34	0.19	0.41	0.23	0.36
e. ***S*-6** methyl	0.36	0.38	0.29	0.32	0.40	0.41	0.30	0.31	0.41	0.54

[a] Photochemically initiated polymer with acetonitrile used as the porogen. [b] HPLC performed using acetonitrile as eluent.

with the polymer matrix. A close look at the corrected retention volumes (k') of the various derivatives indicates that the *R*-enantiomers, with a chiral mismatch to the imprint cavity, have narrowly spread corrected retention volumes (k'_R) that are mostly indicative of the relative polarities of the molecules (Table 2). Their order of elution is not influenced by the choice of the imprint molecule. However, the corrected retention volumes of the matching *S*-enantiomers (k'_S) are strongly dependent on the imprint molecule and order themselves according to a combination of specific and nonspecific matrix effects. *The* α *values are largely determined by the changes in* k'_S *relative to a nearly constant* k'_R. This trend is shown graphically in Figure 3, which plots the selectivity factor and the capacity factors for each benzodiazepine derivative analyzed using the ***S*-8** imprinted polymer. This plot is typical of the other MIPs that were investigated. As the fit between the imprint cavity and the analyte molecule improves, the selectivity and therefore the separation factor increases. The repeated selectivity of MIPs for the template molecule over so many structurally similar species is striking.

It was found that changing the composition of the mobile phase from pure acetonitrile to binary mixtures of acetonitrile and chloroform caused a bimodal change in the capacity factor of the template molecule (Figure 4). This behavior is a general observation that has been observed with a variety of solutes

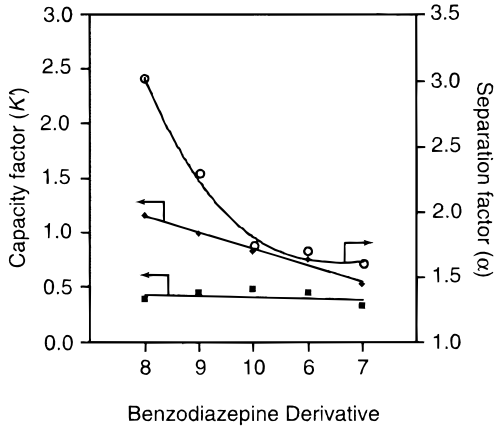

Figure 3. Graphical representation of capacity factor and separation factor data for benzodiazepine derivatives injected onto a HPLC column packed with ***S*-(8)** (benzyl) benzodiazepine imprinted polymer: k'_R (■), k'_s (◆), α (○).

and chiral stationary phases.[10,11] The phenomena has been

(10) Funk, M.; Frank, H.; Oesch, F.; Platt, K. L. *J. Chromatogr. A* **1994**, *659*, 57.

(11) (a) Pescher, P.; Caude, M.; Rosset, R. *J. Chromatogr.* **1986**, *371*, 159. (b) Siret, L.; Tambuté, A.; Caude, M.; Rosset, R. *J. Chromatogr.* **1990**, *498*, 67.

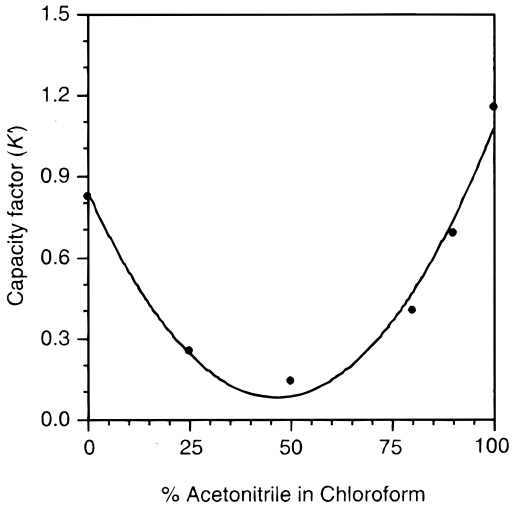

Figure 4. Effect of eluent composition on the capacity factor (●) of ***S*-(8)** obtained from an HPLC column packed with ***S*-(8)** imprinted polymer.

Table 3. Capacity Factors on an ***S*-8** (Benzyl) Benzodiazepine MIP Column[a,b]

molecule	k'	molecule	k'
(*S*)-8 benzyl	1.15	**(*R*)-9** hydroxy benzyl	0.44
(*S*)-9 hydroxy benzyl	0.99	**(*R*)-6** methyl	0.44
(*S*)-10 indolyl	0.82	**(*R*)-8** benzyl	0.38
(*S*)-6 methyl	0.75	**(*R*)-7** isopropyl	0.32
(*S*)-7 iIsopropyl	0.52	(±)-Lormetazepam	0.29
(±)-Lorazepam	0.51	benzylamine	0.27
(*R*)-10 indolyl	0.47	flunitrazepam	0.19

[a] Photochemically initiated polymer with acetonitrile used as the porogen. [b] HPLC performed using acetonitrile as eluent.

attributed to the intermediate polarity of the stationary phase with respect to the solvents being used.[10] In acetonitrile, the higher capacity factor is contributed to by nonpolar interactions with the stationary phase. This interaction is reduced by addition of a nonpolar solvent, chloroform. In pure chloroform, the interaction with the stationary phase is polar in nature, and therefore is reduced by addition of the polar solvent acetonitrile.

Table 3 shows the capacity factors (k') for a variety of substances obtained using a MIP imprinted with benzodiazepine ***S*-8.** As would be expected, the template benzodiazepine had the highest affinity for the stationary phase.

The *S* forms of other benzodiazepines show slightly lower affinity for these stationary phases. As mentioned earlier, this decrease in capacity factor most likely results from the mismatch of the side chain of the amino acid portion of the molecules with the cavity formed around the template molecule. The fact that all of the *S* enantiomers are retained over the *R* enantiomers indicates that the perturbation caused by the inversion of the stereocenter has a more profound effect on the binding energy than the structural changes associated with different side chains.[12]

The *R* enantiomers of the benzodiazepines appear at significantly lower capacity factors. This highlights the importance of proper fit into the chiral cavity created by imprinting an *S* enantiomer. It is important to note that selectivity between the enantiomers of the isopropyl and methyl derivatives is achieved. This demonstrates the wide range of structural variation that is

Scheme 2

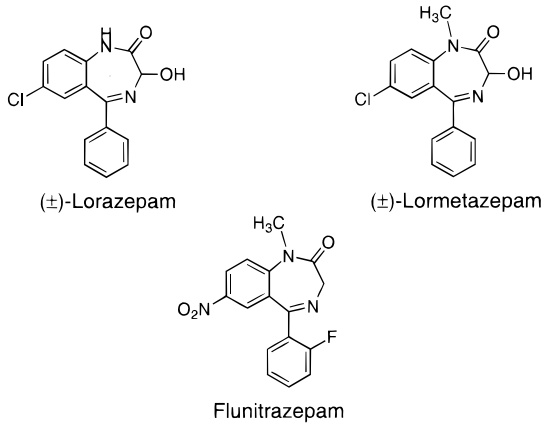

possible. Also in this group is the racemic mixture of Lorazepam that elutes as a somewhat broadened peak.

The third block of compounds includes racemic Lormetazepam, which is structurally related to Lorazepam with the exception of a methyl group on the amide nitrogen. Flunitrazepam, while lacking a chiral center, also has the *N*-methyl group and different substituents on the aromatic rings. The difference in retention between the *N*-methyl containing compounds and the non-methylated compounds deserves further comment. Having already established the chiral center as a specific recognition element, the amide nitrogen is implicated as a secondary site for interaction with the matrix. If hydrogen bonding with the carboxylic acid groups of the matrix contributes to the recognition, the methylation of the amide nitrogen would severely disrupt the binding interaction. This seems to be the cause of the lower k' in Lormetazepam compared to that of Lorazepam, since the rest of the molecule is identical. The fact that Flunitrazepam, with no pendant chiral residue, has retention similar to that of Lormetazepam suggests that the amide hydrogen is a significant determinant of binding.

We currently have no pharmacological data on the amino acid functionalized benzodiazepines. However, it is of interest to note that while Lorazepam is an anxiolytic drug, Lormetazepam and Flunitrazepam are classified as hypnotic drugs.[13] All benzodiazepines are CNS depressants and act by binding to a receptor for γ aminobutyric acid ($GABA_A$) in the brain and allosterically modulating its activity.[14] It is known that many subtypes of $GABA_A$ receptors exist, but as yet no association of subtypes with physiological effects has been made. It has been hypothesized that the wide range of benzodiazepine pharmacological effects is due to the complex interplay of different drugs preferentially binding different $GABA_A$ receptor subtypes.[14]

The fact that the hypnotic drugs elute differently than the anxiolytic benzodiazepine suggests that MIPs might be able to differentiate between molecules which bind to different subtypes of receptors as well. Using a MIP model of a specific receptor subtype could greatly increase the speed and ease with which compounds could be developed having high binding specificity for that individual receptor. In addition to obtaining new, more specific drugs, we may also be able to learn more about the likely composition and pharmacology of the $GABA_A$ receptor subtypes.

In summary, molecularly imprinted polymers were prepared that can be used to separate enantiomers of a series of

(12) At this time we have no information about the solution conformations of the benzodiazepines being studied and what effect, if any, that may have on recognition.

(13) Budavari, S., Ed. *The Merck Index*, 11th ed.; Merck & Co., Inc.: Rahway, NJ, 1989; pp 5456 and 5458.

(14) Sieghart, W. *J. Psychiatr. Neurosci.* **1994**, *19*, 24−29.

benzodiazepine molecules. A detailed HPLC analysis of binding properties using MIP stationary phases showed significant dependence on the chiral match or mismatch with the shape of the imprinted binding site. These results demonstrate the ability of MIPs to discriminate between enantiomers of molecules in favor of the imprinted absolute configuration, even as the structural homology between the enantiomers and the original template decreases.

The reported results indicate that these synthetic benzodiazepine receptors may serve as crude mimics of the natural receptor. While MIPs used as synthetic drug receptors may not mimic protein microenvironments, they may nevertheless prove useful for screening large libraries of compounds for molecules with similar or related affinities. As molecular structure is key to reactivity, it is possible that MIPs may be able to sort molecules based on their pharmacological properties. In this specific case, the response of various drugs to a set of imprinted polymers may provide clues to their binding of $GABA_A$ receptors, providing a new technique for use in developing better, more selective pharmaceuticals.

Experimental Section

Instrumentation. Proton nuclear magnetic resonance spectra (^{1}H NMR) were recorded at 500 MHz on Bruker spectrometers. Carbon nuclear magnetic resonance spectra (^{13}C NMR) were recorded on Bruker spectrometers at 125.8 MHz. Infrared spectra (IR) were measured on an Analect RFX-40 FTIR spectrometer. HPLC analyses were performed with a Shimadzu LC-10AS dual pump gradient solvent delivery system equipped with an SPD-10AV UV/Vis detector and a Hewlett-Packard 3396A integrator. A Thomas-Hoover capillary melting point apparatus was used to observe uncorrected melting points. High-resolution mass spectra (EI, 70 eV or CI, isobutane or ammonia) were obtained on a VG 7070E high-resolution mass spectrometer or Fisons Autospec mass spectrometer. Optical rotations were obtained using a JasCo DIP-360 digital polarimeter. UV irradiation experiments utilized a Hanovia medium-pressure mercury arc lamp.

General Procedures. All solvents were distilled from drying agents (CaH_2 or Na/benzophenone) just before use. Ethylene glycol dimethacrylate (EGDMA, Aldrich) was distilled under reduced pressure (10 mmHg, 60 °C). Methacrylic acid (MAA, Aldrich) was distilled over CaH_2 (10 mmHg, 80 °C). AIBN (Aldrich) was recrystallized from methanol. Glassware was cleaned by soaking in an alcoholic KOH solution overnight and rinsing with water; glassware was oven dried overnight. All reactions were run under a N_2 atmosphere. Volatile solvents were removed under reduced pressure using a Büchi rotary evaporator. Thin-layer chromatography was run on precoated plates of silica gel with a 0.25 mm thickness containing 60F-254 indicator (Merck). Column chromatography was run using 230−400 mesh silica gel (Merck).

General Procedure for Molecularly Imprinted Polymer Synthesis. A solution of ethylene glycol dimethacrylate (3.47 g, 17.5 mmol), methacrylic acid (0.203 g, 2.40 mmol), and AIBN (0.033 g, 0.20 mmol) in acetonitrile or chloroform (4.5 mL) was deoxygenated using nitrogen gas for 15 min. Additional solvent was added to bring the volume of the solution to its initial level. The appropriate enantiomer of benzodiazepine derivative (**6**−**10**, 0.20 mmol) was added and the solution was divided between two 20 mL flame-dried scintillation vials. After further deoxygenating (5 min) the vials were sealed. The polymerizations were initiated photochemical by a mercury arc UV light source at 0 ± 2 °C and allowed to proceed for 12 h under constant irradiation. After crushing, the polymers were extracted with methanol for 36 h, then dried under vacuum. The polymers were further crushed using a mortar and pestle and sieved to isolate the 25−38 μm particles for use in chromatographic experiments.

A slurry was made of the 25−38 μm particles in acetonitrile. This slurry was forced into 4.6 mm i.d. × 10 cm stainless steel HPLC columns using a stainless steel slurry reservoir and a Shimadzu LC-10AS solvent delivery system.

General Procedure for the Preparation of 1−5. To a stirred solution of 2-amino-5-chlorobenzophenone (0.838 g, 3.60 mmol) and the particular *N*-Boc-amino acid (3.3 mmol) in either methylene chloride (5 mL, *N*-Boc-alanine and *N*-Boc-valine) or tetrahydrofuran (5 mL, *N*-Boc-tryptophan, *N*-Boc-phenylalanine, *N*-Boc-tyrosine) was added dicyclohexylcarbodiimide (DCC) (0.746 g, 3.6 mmol) in methylene chloride (5 mL) dropwise, over 30 min at 0 °C. The reaction mixture was stirred an additional 8 h at room temperature. The dicyclohexyl urea formed was filtered off and the filtrate concentrated. The crude products were purified as described below.

General Procedure for the Preparation of 6−10. To a stirred solution of the appropriate benzophenone (**1**−**5**, 2.0 mmol) in chloroform (50 mL) at room temperature was bubbled hydrogen chloride gas slowly. After 20 min, the bubbling was stopped and the solution was stirred overnight at room temperature. The reaction mixture was washed with saturated sodium bicarbonate solution (2×, 50 mL) and water (2×, 50 mL). The organic layer was dried ($MgSO_4$) and concentrated. The residual oil was dissolved in methanol−water (1:1, 30 mL) and the pH was adjusted to 8.5 by the addition of sodium hydroxide (1 N). The reaction mixture was stirred for 10 h at room temperature. The solution was concentrated and water (50 mL) was added. The solution was extracted with CH_2Cl_2 (3 × 50 mL) and the organic layer was dried ($MgSO_4$) and concentrated. The crude products were purified as described below.

2-*N*-(*N*′-Boc-alanyl)amino-5-chlorobenzophenone (*R*-1 and *S*-1). Recrystallization of the crude product from cyclohexane afforded **1** (1.088 g, 82%). Mp 150−152 °C; ^{1}H NMR ($CDCl_3$) δ 11.19 (s, 1 H), 8.62 (d, J = 8.6 Hz, 1 H), 7.68 (d, J = 7.90 Hz, 2 H), 7.61 (t, J = 6.96 Hz, 1 H), 7.52−7.48 (m, 4 H), 5.10 (br s, 1 H), 4.31 (br s, 1 H), 1.46 (d, J = 7.1 Hz, 3 H), 1.41 (s, 9 H); ^{13}C NMR ($CDCl_3$) δ 197.8, 172.0, 155.2, 138.4, 137.7, 133.7, 132.8, 132.5, 129.8, 128.4, 127.4, 124.9, 122.9, 80.2, 51.6, 28.2, 18.4 ppm; IR (KBr, cm^{-1}) 3321, 2979, 2933, 1647, 1597; HRMS calcd for $C_{21}H_{23}N_2ClO_4$ 402.1346, found 402.1334; $[\alpha]^{26}_D$(***R*-1**) = +49.9 (*c* 1.15, $CHCl_3$), $[\alpha]^{26}_D$(***S*-1**) = −49.3 (*c* 0.965, $CHCl_3$).

2-*N*-(*N*′-Boc-valyl)amino-5-chlorobenzophenone (*R*-2 and *S*-2). Flash column chromatography (CH_2Cl_2) afforded a colorless oil. Flash column chromatography of this oil using 10:5:1 petroleum ether/CH_2Cl_2/Et_2O provided **2** (0.925 g, 65%). Mp 106−108 °C; ^{1}H NMR ($CDCl_3$) δ 11.21 (s, 1 H), 8.66 (d, J = 9.7 Hz, 1 H), 7.69 (d, J = 8.3 Hz, 2 H), 7.63 (t, J = 7.5 Hz, 1 H), 7.53−7.50 (m, 4 H), 5.10 (br d, J = 7.6 Hz, 1 H), 4.19 (br s, 1 H), 2.35 (m, 1 H), 1.42 (s, 9 H), 1.03 (d, J = 6.9 Hz, 3 H), 0.94 (d, J = 6.9 Hz, 3 H); ^{13}C NMR ($CDCl_3$) δ 198.0, 171.1, 156.8, 138.5, 137.8, 133.9, 132.9, 132.7, 129.9, 128.5, 127.5, 124.8, 122.9, 80.2, 31.0, 30.8, 28.3, 19.4, 17.4; IR (KBr, cm^{-1}) 3320, 2969, 2931, 1695, 1506; HRMS calcd for $C_{23}H_{27}N_2ClO_4$ 430.1659, found 430.1662; $[\alpha]^{26}_D$(***R*-2**) = +47.2 (*c* 0.93, $CHCl_3$), $[\alpha]^{26}_D$(***S*-2**) = −46.4 (*c* 0.85, $CHCl_3$).

2-*N*-(*N*′-Boc-phenylalanyl)amino-5-chlorobenzophenone (*R*-3 and *S*-3). Flash column chromatography (10:1 CH_2Cl_2/Et_2O) afforded **3** (0.978 g, 62%). Mp 136−138 °C; ^{1}H NMR ($CDCl_3$) δ 10.92 (br s, 1H), 8.62 (d, J = 8.9 Hz, 1 H), 7.64 (m, 3 H), 7.51 (m, 4 H), 7.20 (m, 4 H), 7.07 (m, 1 H), 5.04 (br s, 1 H), 4.52 (br s, 1 H), 3.16 (d, J = 6.2 Hz, 2 H), 1.38 (s, 9 H) ppm; ^{13}C NMR ($CDCl_3$) δ 197.4, 170.7, 155.2, 138.0, 137.6, 136.1, 133.7, 132.8, 132.4, 129.9, 129.1, 128.7, 128.4, 127.6, 127.0, 125.0, 122.9, 80.4, 57.0, 38.3, 28.2 ppm; IR (KBr, cm^{-1}) 2940, 1672, 1508, 1243, 1128; HRMS calcd for $C_{27}H_{27}N_2ClO_4$ 478.1659, found 478.1658; $[\alpha]^{26}_D$(***R*-3**) = +52.1 (*c* 1.27, $CHCl_3$), $[\alpha]^{26}_D$(***S*-3**) = −52.8 (*c* 1.30, $CHCl_3$).

2-*N*-(*N*′-Boc-tyrosyl)amino-5-chlorobenzophenone (*R*-4 and *S*-4). Flash column chromatography (10:1 CH_2Cl_2/Et_2O) afforded **4** (1.109 g, 68%). Mp 156−158 °C; ^{1}H NMR ($CDCl_3$) δ 10.93 (s, 1 H), 8.59 (d, J = 9.0 Hz, 1 H), 7.65 (d, J = 7.3 Hz, 1 H), 7.62 (t, J = 7.5 Hz, 1 H), 7.50 (m, 4 H), 7.02 (d, J = 8.3 Hz, 2 H), 6.66 (d, J = 8.5 Hz, 2 H), 5.08 (br s, 1 H), 4.45 (br s, 1 H), 3.08 (br s, 2 H), 1.38 (s, 9 H) ppm; ^{13}C NMR ($CDCl_3$) δ 197.6, 170.9, 155.3, 154.9, 138.0, 137.7, 133.8, 132.9, 132.5, 130.3, 129.9, 128.5, 127.7, 125.1, 123.0, 115.7, 80.6, 77.5, 57.1, 37.5, 28.2 ppm; IR (KBr, cm^{-1}) 3318, 2932, 1686, 1514, 1250, 1160; HRMS calcd for $C_{27}H_{27}N_2ClO_4$ (M + Na) 517.1506, found 517.1502; $[\alpha]^{26}_D$(***R*-4**) = +58.2 (*c* 0.972 $CHCl_3$), $[\alpha]^{26}_D$(***S*-4**) = −59.0 (*c* 0.965, $CHCl_3$).

2-*N*-(*N*′-Boc-tryptophanyl)amino-5-chlorobenzophenone (*R*-5 and *S*-5). Flash column chromatography (10:1 CH_2Cl_2/Et_2O) afforded **5** (1.197 g, 70%). Mp 150−152 °C; ^{1}H NMR ($CDCl_3$) δ 10.93 (s, 1 H), 8.63 (d, J = 8.9 Hz, 1 H), 7.96 (br s, 1 H), 7.61−7.57 (m, 4 H), 7.51−7.46 (m, 3 H), 7.43 (s, 1 H), 7.19 (d, J = 8.1 Hz, 1 H), 7.11 (t, J = 7.0 Hz, 1 H), 7.04 (m, 2H), 5.17 (br s, 1 H), 5.60 (br s, 1 H), 3.45 (m, 1 H), 3.34 (dd, J = 14.6, 6.1 Hz, 1 H), 1.40 (s, 9 H) ppm; ^{13}C NMR ($CDCl_3$) δ 197.3, 171.4, 155.4, 138.2, 137.6, 136.1, 133.7, 132.8, 132.4, 129.9, 128.3, 127.4, 124.9, 123.0, 122.9, 122.2, 119.6, 118.7, 111.1, 110.1, 80.3, 56.4, 29.7, 28.2 ppm. 24 signals were detected due to coincident signals in the aromatic region; IR (KBr, cm^{-1}) 3336, 2978, 2929, 1698, 1506; HRMS calcd for $C_{29}H_{28}N_3ClO_4$ 517.1768, found 517.1756; $[\alpha]^{26}_D$(***R*-5**) = +81.6 (*c* 1.01, $CHCl_3$), $[\alpha]^{26}_D$(***S*-5**) = −82.0 (*c* 0.91, $CHCl_3$).

7-Chloro-1,3-dihydro-3-methyl-5-phenyl-2*H*-1,4-benzodiazepine-2-one (*R*-6 and *S*-6). Recrystallization from acetone/water (1:1) provided **6** (0.460 g, 81%). Mp 168−170 °C; ^{1}H NMR ($CDCl_3$) δ 8.62 (s, 1 H), 7.53 (d, J = 7.2 Hz, 2 H), 7.51−7.44 (m, 2 H), 7.39 (m, 2 H), 7.34 (d, J = 2.4 Hz, 1 H), 7.10 (d, J = 8.6 Hz, 1 H), 3.75 (q, J = 6.4 Hz, 1 H), 1.75 (d, J = 6.5 Hz, 3 H) ppm; ^{13}C NMR ($CDCl_3$) δ 172.8, 167.8, 138.6, 137.1, 131.7, 130.5, 130.4, 129.7, 128.9, 128.6, 128.3, 122.6, 58.8, 17.0 ppm; IR (KBr, cm^{-1}) 3226, 3135, 2929, 1685, 1608; HRMS calcd for $C_{16}H_{13}N_2ClO$ (M − H) 283.0638, found 283.0639; $[\alpha]^{26}_D$(***S*-6**) = +124.4 (*c* 1.05, $CHCl_3$), $[\alpha]^{26}_D$(***R*-6**) = −123.6 (*c* 0.99, $CHCl_3$).

7-Chloro-1,3-dihydro-3-isopropyl-5-phenyl-2*H*-1,4-benzodiazepine-2-one (*R*-7 and *S*-7). Recrystallization from petroleum ether/CH_2Cl_2 (40:1) provided **7** (0.537 g, 86%). Mp 189−191 °C; ^{1}H NMR ($CDCl_3$) δ 9.29 (s, 1 H), 7.53−7.31 (m, 7 H), 7.14 (2, J = 8.7 Hz, 1 H), 3.11 (d, J = 9.3 Hz, 1 H), 2.78−2.72 (m, 1 H), 1.21 (d, J = 6.7 Hz, 3 H), 1.10 (d, J = 6.5 Hz, 3 H) ppm; ^{13}C NMR ($CDCl_3$) δ 170.8, 167.5, 138.8, 137.1, 131.6, 130.5, 130.4, 129.7, 128.8, 128.6, 128.3, 122.6, 69.4, 29.0, 20.3, 19.0 ppm; IR (NaCl, cm^{-1}) 3201, 3104, 2958, 1683, 1606; calcd for $C_{18}H_{16}N_2ClO$ (M − H) 311.0951, found 311.0951; $[\alpha]^{24}_D$(***S*-7**) = +115.4 (*c* 1.05, $CHCl_3$), $[\alpha]^{24}_D$(***R*-7**) = −113.0 (*c* 0.97, $CHCl_3$).

7-Chloro-1,3-dihydro-3-benzyl-5-phenyl-2*H*-1,4-benzodiazepine-2-one (*R*-8 and *S*-8). The residual oil was disolved in methanol and water was added to facilitate precipitation. Flash column chromatography (7:3 Hex/EtOAc) afforded **8** (0.582 g, 80%). Mp 108−110 °C; ^{1}H NMR ($CDCl_3$) δ 9.19 (br s, 1 H), 7.45 (m, 4 H), 7.38 (m, 4 H), 7.32 (t, J = 7.6 Hz, 2 H), 7.23 (m, 2 H), 7.12 (br s, 1 H), 3.79 (t, J = 6.8 Hz, 1 H), 3.62 (br s, 2 H) ppm; ^{13}C NMR ($CDCl_3$) δ 171.9, 168.1, 138.9, 138.6, 137.0, 131.7, 130.5, 130.4, 129.8, 129.7, 128.7, 128.6, 129.3, 128.2, 126.2, 122.8, 64.9, 37.5 ppm; IR (KBr, cm^{-1}) 2940, 2362, 1685, 1605, 1478, 1323; HRMS calcd for $C_{22}H_{17}N_2ClO$ 360.1029, found 360.1017; $[\alpha]^{24}_D$(***S*-8**) = +34.2 (*c* 1.100, $CHCl_3$), $[\alpha]^{24}_D$(***R*-8**) = −33.8 (*c* 1.06, $CHCl_3$).

7-Chloro-1,3-dihydro-3-*p*′-hydroxybenzyl-5-phenyl-2*H*-1,4-benzodiazepine-2-one (*R*-9 and *S*-9). Flash column chromatography (8:2 Hex/EtOAc) followed by recrystallization (Et_2O/cyclohexane) provided **9** (0.603 g, 80%). Mp 139−142 °C; ^{1}H NMR ($CDCl_3$) δ 9.47 (br s, 1 H), 7.44 (m, 4 H), 7.36 (t, J = 7.5 Hz, 2 H), 7.22 (d, J = 2.4 Hz, 1 H), 7.20 (d, J = 8.2 Hz, 2 H), 7.12 (d, J = 8.6 Hz, 1 H), 6.76 (d, J = 8.4 Hz, 2 H), 3.72 (br t, J = 6.5 Hz, 1 H), 3.55−3.44 (m, 2 H) ppm; ^{13}C NMR ($CDCl_3$) δ 171.3, 168.4, 154.3, 136.9, 132.8, 131.5, 132.0, 130.9, 130.6, 130.5, 129.9, 129.7, 128.8, 128.4, 122.8, 115.2, 65.0, 26.9 ppm; IR (NaCl, cm^{-1}) 3230, 2932, 1685, 1608; 1515, 1230; HRMS calcd for $C_{22}H_{18}N_2ClO_2$ (M + H) 377.1057, found 377.1057; $[\alpha]^{24}_D$(***S*-9**) = +27.9 (*c* 1.05, $CHCl_3$), $[\alpha]^{24}_D$(***R*-9**) = −26.2 (*c* 0.97, $CHCl_3$).

7-Chloro-1,3-dihydro-3-(3′-indolyl)methyl-5-phenyl-2*H*-1,4-benzodiazepine-2-one (*R*-10 and *S*-10). Water was added to the reaction mixture to facilitate precipitation. Filtration of the precipitate followed by recrystallization from acetone/water (1:1) provided **10** (0.630 g, 79%). Mp 149−151 °C; ^{1}H NMR ($CDCl_3$) δ 9.70 (s, 1 H), 8.11 (s, 1 H), 7.70 (d, J = 7.8 Hz, 1 H), 7.49−7.33 (m, 7 H), 7.23−7.06 (m, 5 H), 3.86−3.81 (m, 2 H), 3.73−3.66 (m, 1H) ppm; ^{13}C NMR ($CDCl_3$) δ 171.9, 168.0, 138.7, 136.9, 136.0, 131.8, 130.5, 129.7, 128.7, 128.6, 128.3, 127.7, 123.3, 122.7, 121.8, 119.1, 119.0, 112.8, 111.1, 64.2, 26.9 ppm. 21 signals were detected due to coincident signals in the aromatic region; IR (KBr, cm^{-1}) 3411, 3328, 3058, 2927, 1684, 1606; HRMS calcd for $C_{24}H_{18}N_3ClO$ 399.1138, found 399.1129; $[\alpha]^{24}_D$(***S*-10**) = +27.4 (*c* 0.85, $CHCl_3$), $[\alpha]^{24}_D$(***R*-10**) = −25.2 (*c* 1.04, $CHCl_3$).

Acknowledgment. We are grateful to the NIH and NSF for financial support of this work.

JA9926313